The Canadian Mineralogist
Vol. 49, pp. 931-946 (2011)
DOI: 10.3749/canmin.49.4.931

THE INDIUM-BEARING MINERALS OF THE PINGÜINO POLYMETALLIC VEIN SYSTEM, DESEADO MASSIF, PATAGONIA, ARGENTINA

SEBASTIÁN M. JOVIC[§] AND DIEGO M. GUIDO

Consejo Nacional de Investigaciones Científicas y Técnicas (CONICET), Instituto de Recursos Minerales (INREMI), Facultad de Ciencias Naturales y Museo, Universidad Nacional de La Plata, Paseo del Bosque s/n, B1900FWA, La Plata, Argentina

JOAN CARLES MELGAREJO

Departament de Cristal·lografía, Mineralogia i Dipòsits Minerals, Universitat de Barcelona, c/ Martí i Franquès s/n, E–08028, Barcelona, Spain

GERARDO N. PÁEZ, REMIGIO RUIZ AND ISIDORO B. SCHALAMUK

Consejo Nacional de Investigaciones Científicas y Técnicas (CONICET), Instituto de Recursos Minerales (INREMI), Facultad de Ciencias Naturales y Museo, Universidad Nacional de La Plata, Paseo del Bosque s/n, B1900FWA, La Plata, Argentina

ABSTRACT

The Pingüino vein system forms part of the low-sulfidation epithermal mineralization associated with the Deseado Massif, Patagonia, Argentina. The ores are complex, with high tenors of Zn, Pb, Ag, Cd, Au, As, Cu, Sn, W and Bi. The mineralization developed in three stages: 1) an early Cu–As–Sn-(W–Bi–Ag–Au–In) stage (Ps_1), 2) a Zn–Pb-(Ag–In–Cd–Sb) stage (Ps_2), and 3) a late Zn–Cd–In stage (Ps_3). The polymetallic veins show a wide range of indium concentration (3.4 to 1184 ppm In). The highest values were achieved during the Ps_2 stage of mineralization, although significant In anomalies are also present in Ps_1 (up to 159 ppm). Three types of In association can be distinguished, on the basis of a microanalytical study of the ores. Iron-rich sphalerite from Ps_2, volumetrically important at this stage, has very high In contents (up to 2.56 wt.% In), and therefore is the most important carrier of In at Pingüino. Tin minerals (ferrokësterite and cassiterite) in the Ps_1 assemblage are the second carriers in importance in these deposits, and their In contents may attain up to 3.02 wt.%. The third type is represented by greenockite crystals from assemblage Ps_3, which presents important In contents (up to 3.63 wt.%), but these minerals are scarce in the deposit. The presence of high values of In and of Zn, Pb, Ag, Au, Cu, Sn, W and Bi in the polymetallic veins of the Pingüino vein system opens interesting possibilities for mineral exploration in the Deseado Massif.

Keywords: indium, sulfides, epithermal, sphalerite, cassiterite, ferrokësterite, greenockite, Deseado Massif, Argentina.

SOMMAIRE

Le système de veines minéralisées de Pingüino fait partie d'une minéralisation épithermale à faible degré de sulfuration associée au massif de Deseado, en Patagonie, Argentine. Il s'agit de minerais complexes, enrichis en Zn, Pb, Ag, Cd, Au, As, Cu, Sn, W et Bi. La minéralisation s'est développée en trois stades: 1) stade précoce (Ps_1) impliquant Cu–As–Sn-(W–Bi–Ag–Au–In), 2) stade intermédiaire (Ps_2) impliquant Zn–Pb-(Ag–In–Cd–Sb), et 3) stade tardif (Ps_3), avec enrichissement en Zn–Cd–In. Les veines polymétalliques varient grandement dans leur teneur en indium, entre 3.4 et 1184 ppm. Les valeurs les plus élevées ont été atteintes au stade Ps_2 de la minéralisation, quoique des anomalies importantes aient été signalées au stade Ps_1 (jusqu'à 159 ppm). Nous distinguons trois types d'associations de l'indium, suite à notre étude microanalytique des minerais. La sphalérite ferrifère du stade Ps_2, composante prédominante à ce stade, possède une teneur très élevée en indium (jusqu'à 2.56%, poids), et serait donc le minéral hôte le plus important à Pingüino. Viennent ensuite les minéraux d'étain (ferrokësterite et cassitérite) de l'assemblage Ps_1, seconds en importance dans ce gisement; leurs teneurs en indium peuvent atteindre 3.02%. Le troisième hôte en importance est la greenockite, de l'assemblage Ps_3, dont les cristaux peuvent contenir jusqu'à 3.63%, mais ces minéraux sont

§ *E-mail address*: sjovic@inremi.unlp.edu.ar

rares dans ce gisement. La présence de valeurs élevées en In et en Zn, Pb, Ag, Au, Cu, Sn, W et Bi dans les veines polymétalliques du système de Pingüino présente des possibilités intéressantes pour l'exploration minérale dans le massif de Deseado.

(Traduit par la Rédaction)

Mots-clés: indium, sulfures, épithermal, sphalérite, cassitérite, ferrokësterite, greenockite, massif de Deseado, Argentine.

Introduction

The Deseado Massif, located in the province of Santa Cruz in southern Argentinian Patagonia, is characterized by the presence of low-sulfidation epithermal deposits that are spatially, temporally and genetically related to a complex and long-lived (more than 30 Ma) middle to upper Jurassic volcanic event associated with tectonic extension (Guido & Schalamuk 2003). The Deseado Massif is an important Au–Ag producer, with four mines (Cerro Vanguardia, Martha, San José and Manantial Espejo) in operation, as well as an area of intense prospecting activity. Mineralization consists mainly of quartz veins and veinlets, vein stockworks and hydrothermal breccias mainly hosted in Jurassic volcanic rocks. The dominant trend of mineralized veins is NW to WNW, with subsidiary veins oriented NE–SW and E–W. Quartz commonly is massive, brecciated and crustiform, or shows colloform banding, with comb, cockade and lattice-bladed texture. Ore minerals in the quartz veins, commonly less than 1% in volume, mainly consist of pyrite, native gold, acanthite, native silver, sulfosalts of silver, hematite, sphalerite, galena and chalcopyrite. The geochemical signature is characterized by anomalous levels of precious metals (Au–Ag) and locally anomalous contents of As, Sb, Hg, Mo, Pb, Zn, Mn and minor Cu (Guido & Schalamuk 2003).

Pingüino is an atypical area in the Deseado Massif (Guido *et al.* 2005). It is located in the central portion of the region, 40 km to the northwest of the Cerro Vanguardia mine (Fig. 1a). Pingüino is characterized by the presence of two different types of veins: a) early polymetallic sulfide-rich veins, and b) late Ag–Au quartz-rich veins. Geochemical exploration revealed that these sulfide-rich veins are enriched in Zn, Ag, Pb, Au, Cu, Sn, W, Bi and In. One of the most interesting elements, in view of its economic potential, is indium. Our aim in this study is to determine the In-bearing minerals and paragenesis, and to describe the behavior of indium in the polymetallic mineralization of the Pingüino vein system.

Background Information

Indium deposits are rare; unfortunately there is very little information about the potential for this element, which is basic for the industry of solar cells. High indium contents have been noted to date in different types of deposits: metamorphosed sedex deposits (Burke & Kieft 1980), low-temperature Pb–Zn vein-type deposits (Palero-Fernández & Martín-Izard 2005), skarns (Ishihara *et al.* 2006), VHMS and the present-day exhalative equivalents (Binns & Scott 1993, Fouquet *et al.* 1993a, 1993b, Huston *et al.* 1995, Schwarz-Schampera & Herzig 1997, Serranti *et al.* 2002, Benzaazoua *et al.* 2003, Ishihara *et al.* 2006), epithermal veins (Carrillo-Rosúa *et al.* 2008) and polymetallic veins linked with granites (Seifert 1999, Tsushima *et al.* 1999, Lenharo *et al.* 2002, Ishihara *et al.* 2006, Zhang *et al.* 2006, Lerouge *et al.* 2007). Among them, the economically most interesting deposits are probably Sn-bearing Pb–Zn deposits (Qian *et al.* 1998, Zhang *et al.* 2007).

Indium may be encountered worldwide either as indium minerals or disseminated as a trace element in the structure of other minerals. Minerals of indium are extremely rare worldwide, and only a few occurrences have been described to date. The most common species of In minerals are roquesite [$CuInS_2$], laforêtite [$AgInS_2$], indite [$FeIn_2S_4$], petrukite [$(Cu,Fe,Zn)_3(Sn,In)S_4$] and sakuraiite [$(Cu,Fe,Zn,Ag)_3(Sn,In)S_4$]. Indium sulfides have been rarely found in polymetallic Sn-bearing vein-type deposits, generally related with differentiated granite intrusions (Shimizu & Kato 1991, Moura *et al.* 2007). On the other hand, minor quantities of indium may substitute for elements with a similar ionic radius in some base-metal sulfides, specially sphalerite, chalcopyrite (Boorman & Abbott 1967, Kieft & Damman 1990), digenite (Boorman & Abbott 1967), stannite [Cu_2FeSnS_4] (Boorman & Abbott 1967), ferrokësterite–kësterite [$Cu_2(Fe,Zn)SnS_4$] and cassiterite (Plimer *et al.* 1991, Schwarz-Schampera & Herzig 2002, Gorelikova *et al.* 2006).

Geological Setting of the Pingüino Vein System

The oldest rocks in the study area (Fig.1a) are middle to upper Triassic continental sedimentary rocks of El Tranquilo Group (Jalfin & Herbst 1995; Fig. 1b). These are fine to coarse sandstones with volcanic components, which are rhythmically intercalated with siltstones, mudstones, black shales and coal horizons. Stocks of lower Jurassic diorite with associated mafic sills and dikes intrude the Triassic rocks (Jovic 2010). The lower Jurassic Roca Blanca Formation (Herbst 1965) is composed of volcaniclastic sandstones to fine conglomerates, some tuffaceous levels and minor ignimbrite deposits. Basaltic lava flows of the El Piche Formation (Jovic 2010) crop out in the northern sector of the area, and are interbedded within the volcaniclastic rocks

of the Roca Blanca Formation. In the northwestern sector, the sequence is intruded by subvolcanic bodies of porphyritic andesite which have been correlated with the middle Jurassic Cerro León Formation (Panza 1995). A regional domed structure 15 to 20 km in diameter, with associated radial faulting, and localized minor domal structures (<1 km) are recognized in the area. A deep intrusion (1.5 km) was proposed to be responsible for the regional doming and the radial fracture system. The minor domal structures represent local deformation associated with shallow, generally unexposed, plutonic and subvolcanic intrusions. These interpretations have been confirmed by aerial magnetometry survey (Peñalva *et al*. 2008) and mining and oil exploration drill holes (Argentex Mining Corp. 2009, and Cortiñas *et al*. 2005). The El Tranquilo Fault (N325°, 70°ENE) is the principal brittle structure, and is associated, mainly to the east, with secondary extensional faults forming a NW-oriented extensional system with sinistral strike–slip duplexes (Jovic *et al*. 2006).

Structure of the Mineralization in the Pingüino Vein System

The Pingüino vein district is composed by 74 linear km of veins that infill fault systems trending NW and ENE. Veins are hosted in Triassic continental sedimentary rocks and lower Jurassic volcaniclastic and volcanic rocks; they are genetically and spatially related to the lower Jurassic dioritic intrusions and the middle Jurassic andesitic subvolcanic porphyries (Jovic 2010, Jovic *et al*. 2011a). Veins are present in the three recognized systems of faults: El Tranquilo (T) fault-vein system (N330°–N325°), Marta (M) fault-vein system (N300°–N310°), and Kasia (K) fault-vein system (N260°–N250°). The T and M systems host the most important veins: Marta Norte, Ana, Marta Noroeste, Savary, Marta Este, Marta Oeste, Marta Centro, Ivonne Norte, Marta Sur, Ivonne and Ivonne Sur. The K system also contains mineralized veins, such as Kasia, Kae and Kalia (Fig. 1b).

The deposits are characterized by the presence of two types of veins: a) early polymetallic sulfide-rich veins and b) late argentiferous quartz-rich veins. These late quartz-rich Ag–Au veins cross-cut the early polymetallic sulfide-rich veins, thus providing evidence of the overlapping of the two different styles of mineralization in the same fault system. The quartz-rich veins have similar characteristics to the typical low-sulfidation type of mineralization from the Deseado Massif (Jovic 2010, Jovic *et al*. 2011a) and are not discussed here further.

Polymetallic Mineralization

The polymetallic mineralization is characterized by the presence of massive and banded sulfide veins and vein breccias (Figs. 2a, b) up to 13 m in width. Ore shoots, developed in the primary zones up to 400 m deep, are of high grade (Argentex Mining Corporation, 2009). The ore's composition reveals the presence of high values of Zn, Ag, Pb, Au, Cu, Sn, W and Bi in the sulfide-rich veins; indium show a wide range of concentration between 3.4 to 1184 ppm (Jovic *et al*. 2011b). The association of major and minor elements reflects two different clusters, one characterized by anomalous values of Au, Cu, In, Sn, W and Bi, and the other with high values of Zn, Pb, Ag, In, Cd and Sb (Jovic *et al*. 2011b).

Recently, Jovic *et al*. (2011a) defined three main stages of mineralization (Fig. 3). The mineralogy of the different stages was determined by optical microscopy, scanning electron microscopy and quantitative electron-microprobe analysis. At all stages, the ore minerals tend to infill open cavities, and therefore they are idiomorphic.

The early stage (Ps_1) is characterized by a complex paragenesis, composed mainly of idiomorphic pyrite crystals, zoned arsenopyrite crystals up to 1 cm across (Fig. 4a), and hypidiomorphic crystals of chalcopyrite between 10 μm and 2 mm. Cassiterite is present as allotriomorphic and idiomorphic crystals up 200 μm across that fill fractures (Fig. 4b) or cross-cut pyrite (Fig. 4c), arsenopyrite and chalcopyrite. Radial aggregates of idiomorphic crystals of hübnerite [$MnWO_4$] (<1 mm) are associated with the cassiterite (Fig. 4b). Ferrokësterite [$Cu_2(Fe,Zn)SnS_4$] replaces cassiterite (Figs. 4b, c and d), and is in turn replaced by stannite [Cu_2FeSnS_4] (Fig. 4e). Very fine-grained (<50 μm) acicular and prismatic Ag–Bi, Ag–Pb–Bi, Pb–Bi sulfosalts like aramayoite [$Ag_3Sb_2(Bi,Sb)S_6$], owyheeite [$Ag_3Pb_{10}Sb_{11}S_{28}$], ourayite [$Ag_3Pb_4Bi_5S_{13}$], giessenite [$(Cu,Fe)_2Ag_{26.4}(Bi,Sb)_{19.6}S_{57}$] and izoklakeite [$Pb_{26.4}(Cu,Fe)_2(Sb,Bi)_{19.6}S_{57}$] are present late at this stage (Fig. 4f). Minor amounts of bournonite [$CuPbSbS_3$] and quartz were also recognized. This stage is best represented in the Ivonne vein (Jovic *et al*. 2005, Crespi 2006).

The second stage (Ps_2) is characterized by a Zn, Pb, Ag, In, Cd and Sb paragenesis, where Ps_1 minerals were brecciated and replaced mainly by banded sphalerite and galena (Figs. 5a, b). The sphalerite is black in hand specimen; in polished section, the crystals are allotriomorphic to idiomorphic and up to 2 cm across. Some crystals contain abundant inclusions of chalcopyrite that range from minute blebs a few μm or less in size to small irregular grains 20 to 50 μm in size. In some sphalerite grains, an irregular and widespread distribution of chalcopyrite is characteristic of the so-called "chalcopyrite disease" described by Barton & Bethke (1987). Minor late ferrokësterite crystals fill fractures in sphalerite. Galena is very abundant and present in irregular masses or as idiomorphic crystals a few centimeters across; it is intergrown with sphalerite. Grains of hypidiomorphic tetrahedrite and freibergite between 100 and 500 μm across (Fig. 5c), allotriomorphic argentotennantite (<20 μm) and Pb–Ag sulfosalts (<20

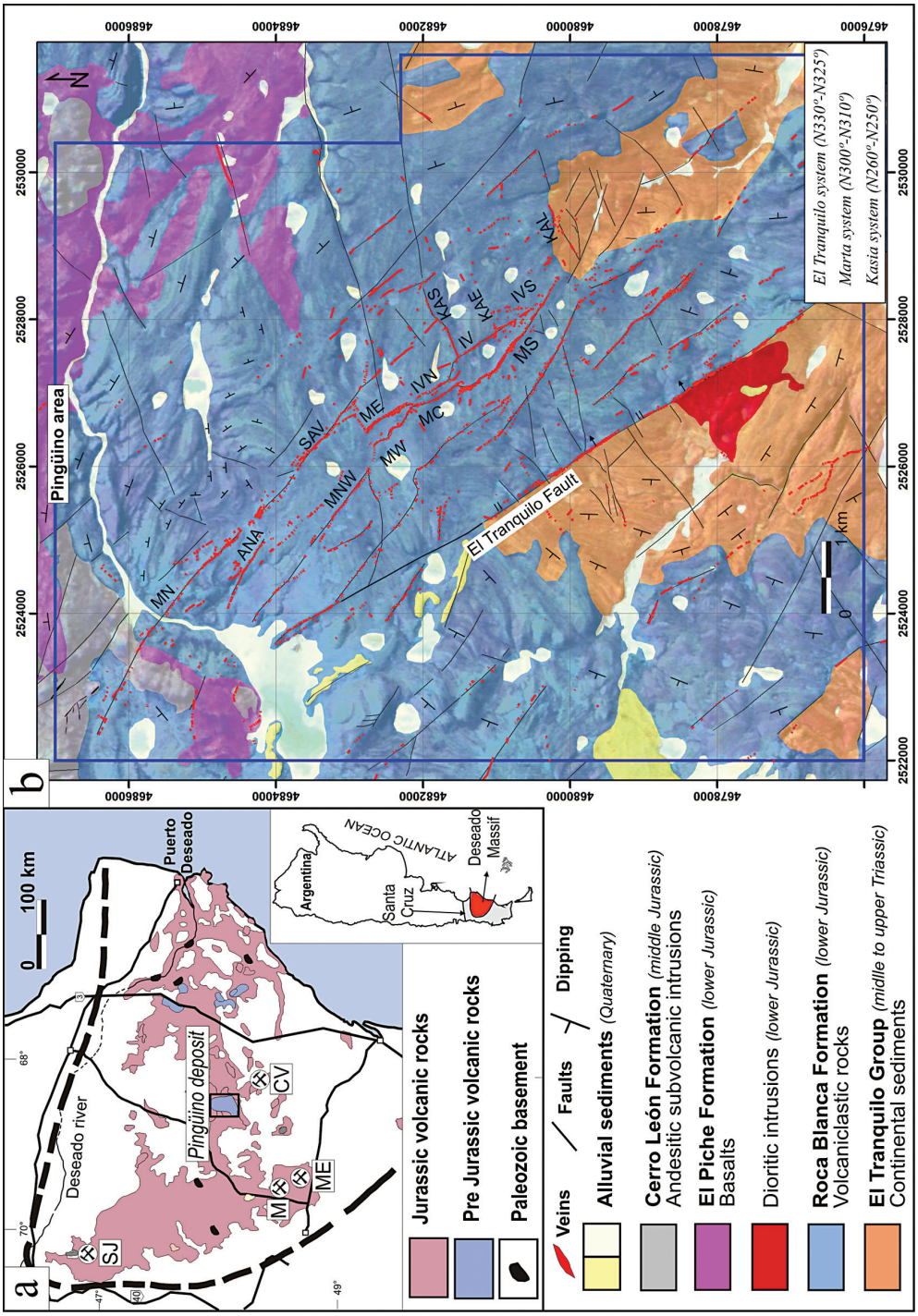

FIG. 1. a) Summary geological map of the Deseado Massif showing the location of the Pingüino claim and the active mines. CV: Cerro Vanguardia mine, M: Martha mine, ME: Manantial Espejo mine, SJ: San José mine. b) Geological and mineralization map of the Pingüino claim. MN Marta Norte, ANA Ana, SAV Savary, MNW Marta Noroeste, ME Marta Este, MW Marta Oeste, MC Marta Centro, IVN Ivonne Norte, IV Ivonne, KAS Kasia, MS Marta Sur, IVS Ivonne Sur, KAL Kalia, veins.

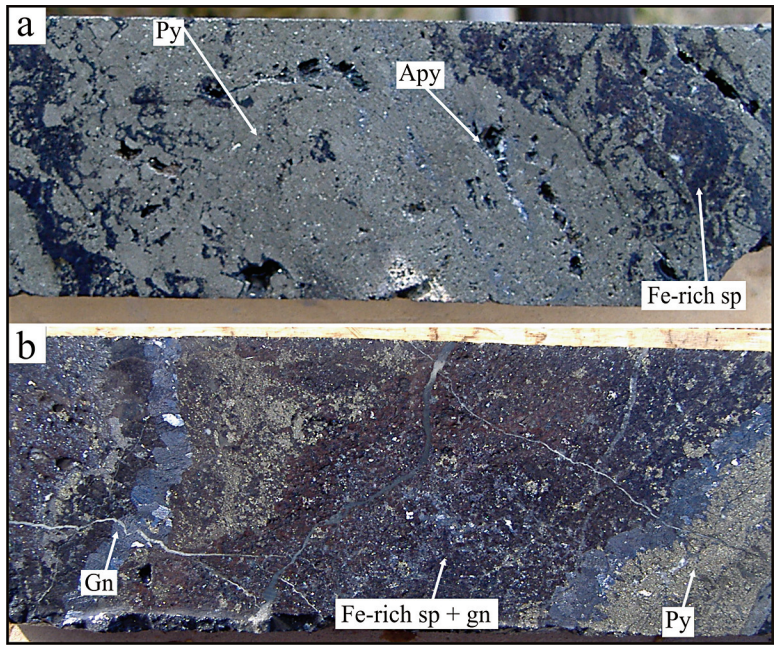

FIG. 2. a) Sulfide veins HQ diameter (65 mm) drill-core samples. Pyrite (Py) and arsenopyrite (Apy) crosscut by Fe-rich sphalerite (Sp) and galena (Gn); Ivonne vein (DDH–102; 53.3 meters below collar). b) Banded Fe-rich sphalerite and galena breccia with pyrite clasts; Marta Centro vein (DDH–53, 54.2 meters below collar).

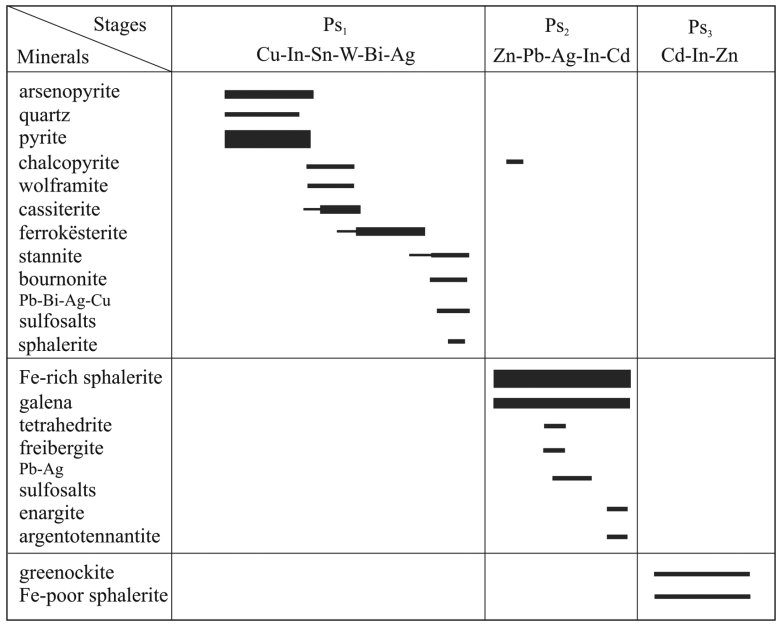

FIG. 3. Paragenetic diagram of the sulfide veins from the Pingüino deposit. Polymetallic stage 1 (Ps_1), polymetallic stage 2 (Ps_2), polymetallic stage 3 (Ps_3).

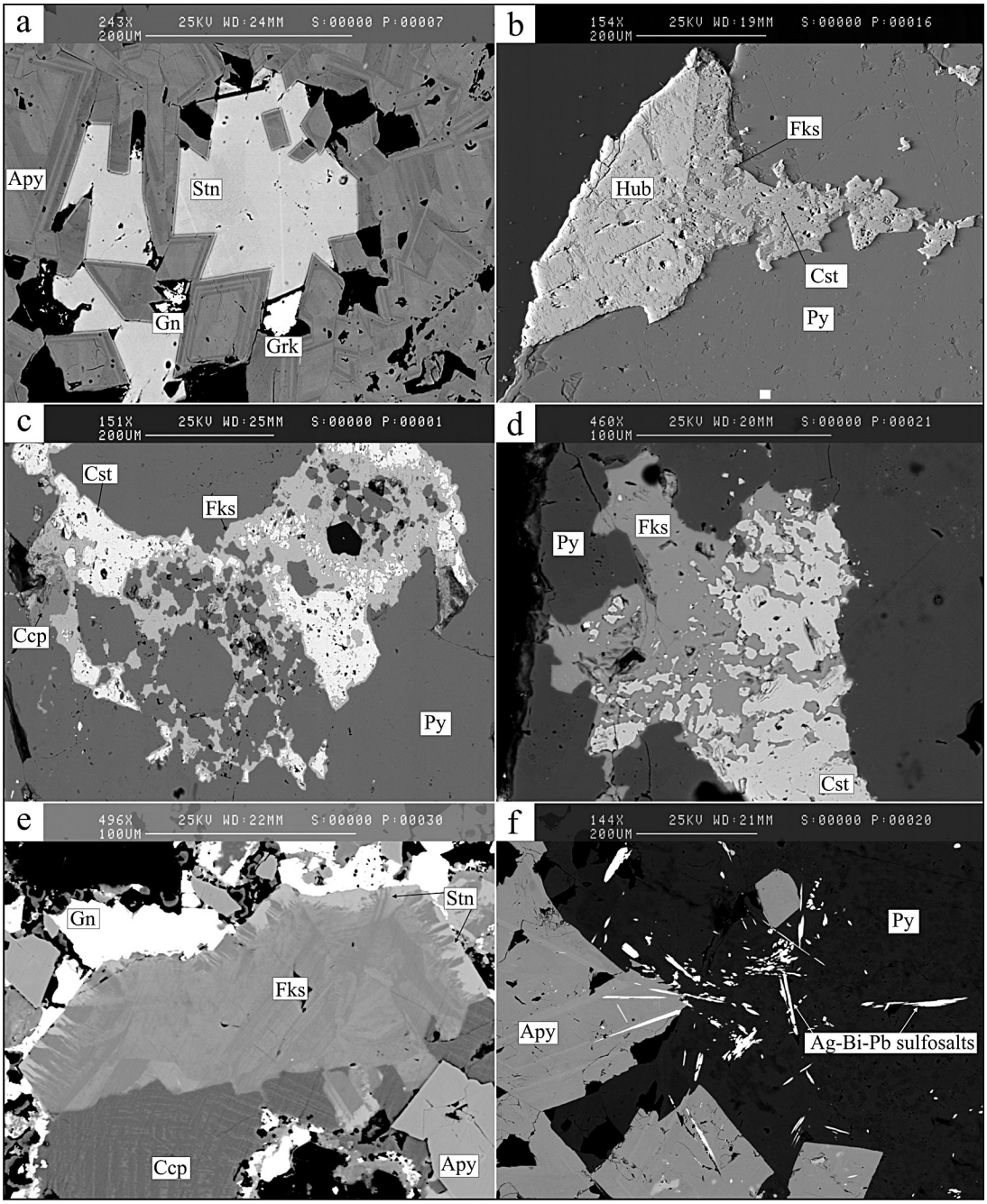

FIG. 4. Back-scattered images from Ps_1 in the Ivonne vein. a) Zoned arsenopyrite (Apy) and stannite (Stn) crystals filling cavities. b) Cassiterite (Cst), ferrokësterite (Fks) and hübnerite (Hub) cross-cutting pyrite (Py). c) Pyrite (Py) and chalcopyrite (Ccp) crystals brecciated by cassiterite (Cst) and ferrokësterite (Fks). d) Ferrokesterite (Fks) replacing cassiterite (Cst). e) Zoned ferrokësterite (Fks) crystal with stannite (Stn) borders. f) Acicular Ag–Bi–Pb sulfosalts crystals; Grk: greenockite.

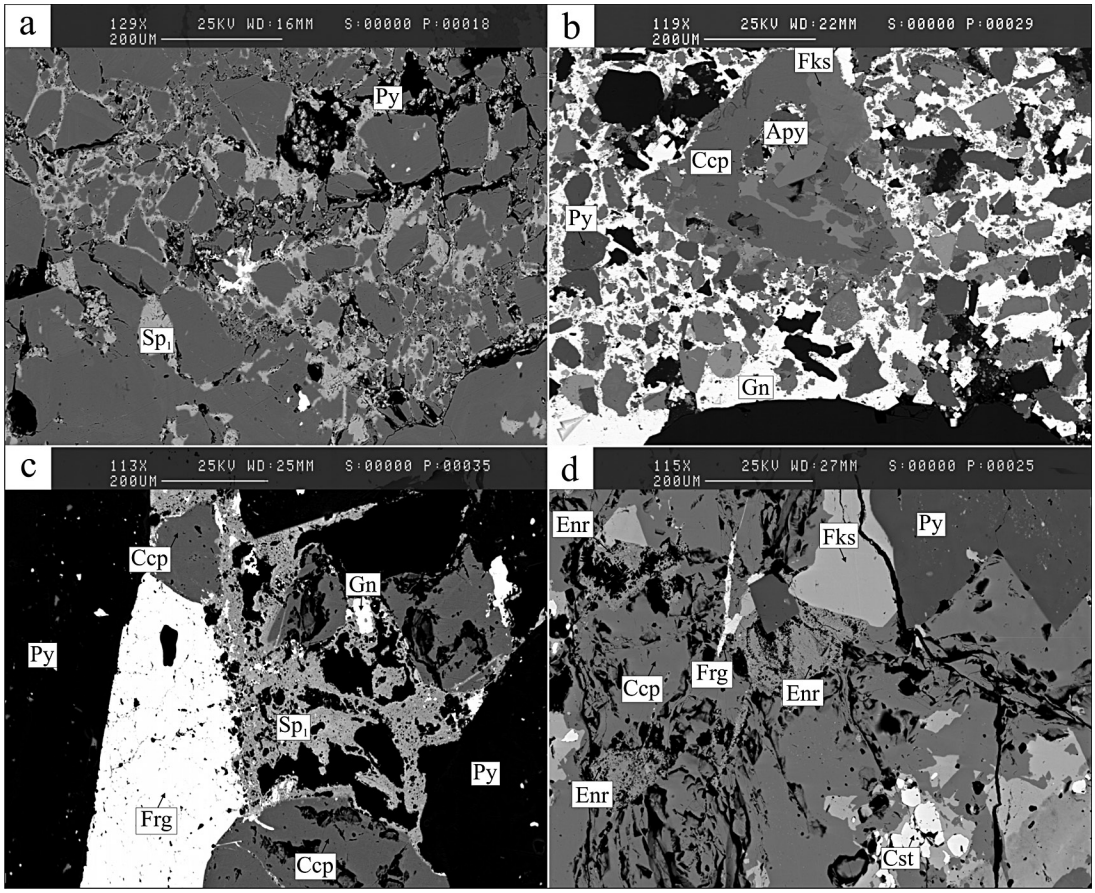

FIG. 5. Back-scattered images from Ps_2 in the Marta Centro vein. a) Brecciated pyrite (Py) is cemented by Fe-rich sphalerite (Sp_1). b) Galena (Gn) breccia with pyrite (Py), chalcopyrite (Ccp) and ferrokësterite (Fks) clasts. c) Fe-rich sphalerite (Sp_1), freibergite (Frg) and galena (Gn) cross-cutting pyrite (Py) and chalcopyrite (Ccp) crystals. d) Enargite (Eng) and freibergite (Frg) cross-cutting Ps_1 minerals.

μm) are present at this stage. Minor late grains (<50 μm) of enargite are present in the cleavage planes of galena or as irregular masses related with freibergite (Fig. 5d). The Ps_2 assemblage is best developed in the Marta Centro vein (Jovic *et al*. 2005, Crespi *et al*. 2006).

A third stage of mineralization (Ps_3) was recognized only at the microscopic scale. It is characterized by an interbedding of botryoidal bands made up by Fe-poor sphalerite and greenockite, followed by tiny (<25 μm) idiomorphic crystals of greenockite (Figs. 6a, b). This stage is represented in the Ivonne and Marta Centro veins (Jovic *et al*. 2005, Crespi 2006).

Geochemical analyses show, for the Ivonne vein (dominantly Ps_1), concentrations of indium up to 159 ppm that strongly correlate with the amounts of Sn (r = 0.77), Sb (r = 0.77) and Ag (r = 0.70). The highest values of indium are present in Marta Centro vein (dominantly Ps_2), with up to 1184 ppm; they have a high correlation with Zn (r = 0.77) and Cd (r = 0.80), but also with Sn (r = 0.70) (Jovic *et al*. 2011b).

INDIUM MINERALOGY

In order to determine the distribution of indium in specific minerals, indium-rich samples from the Ivonne vein (Ps_1 and Ps_3) and the Marta Centro vein (Ps_2 and Ps_3) were selected for detailed mineralogical studies, quantitative electron-microprobe analyses and image analysis.

Analyses of minerals in polished thin sections were carried out at the Serveis CientíficoTècnics, Universitat de Barcelona, Spain, with a Cameca SX50 electron microprobe equipped with four wavelength-dispersive spectrometers and an energy-dispersive spectrometer. The analytical conditions for the study of ore minerals were: S, pyrite ($K\alpha$, PET); Fe, pyrite ($K\alpha$, LIF); Cu,

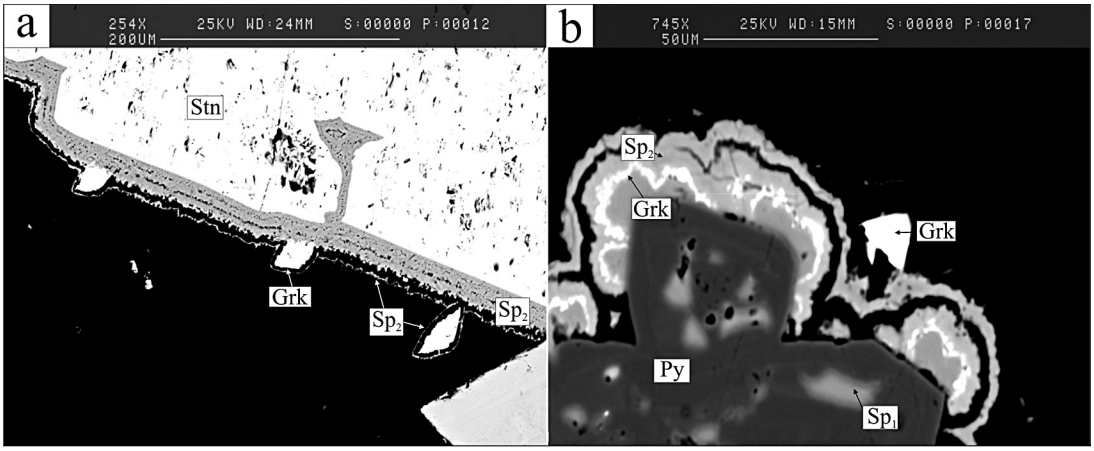

FIG. 6. Back-scattered images from Ps_3 in the Ivonne vein. a) Stannite (Stn) and idiomorphic greenockite (Grk) crystals are surrounded by botryoidal banded Fe-poor sphalerite (Sp_2). b) Botryoidal banded Fe-poor sphalerite (Sp_2) and greenockite (Grk) surrounding a pyrite (Py) crystal with Fe-rich sphalerite (Sp_1) and an idiomorphic greenockite (Grk) crystal over the botryoidal bands.

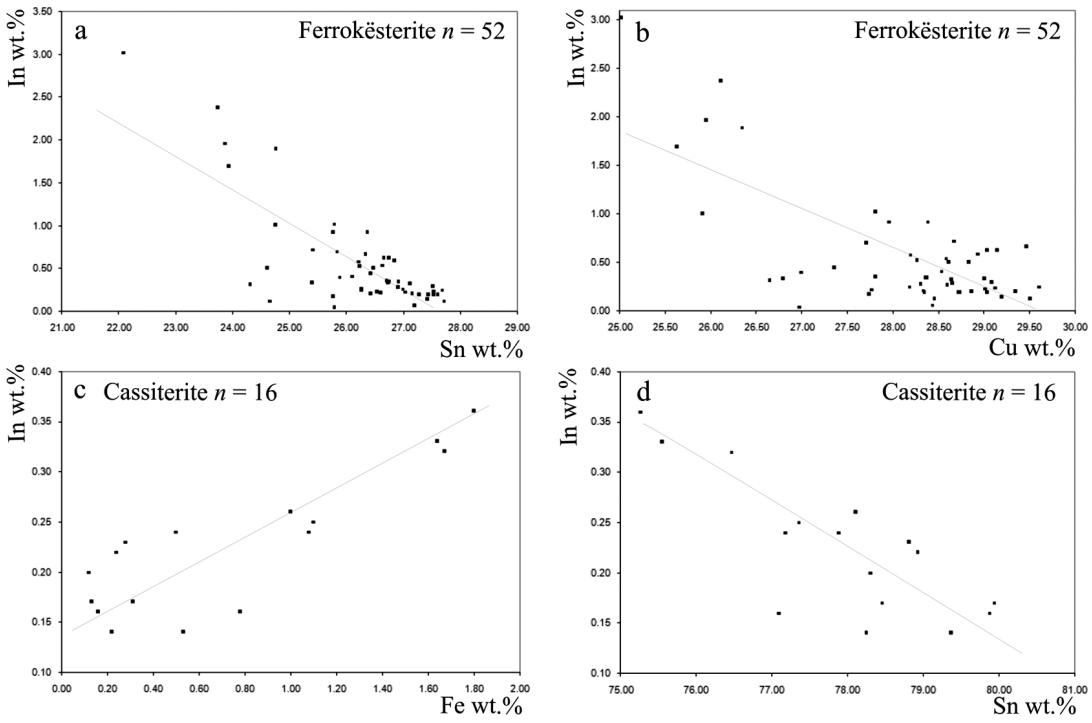

FIG. 7. Binary diagrams of Sn–In and Cu–In proportions in ferrokësterite and Fe–In and Sn–In compositions of cassiterite. *n*: number of electron-microprobe measurements.

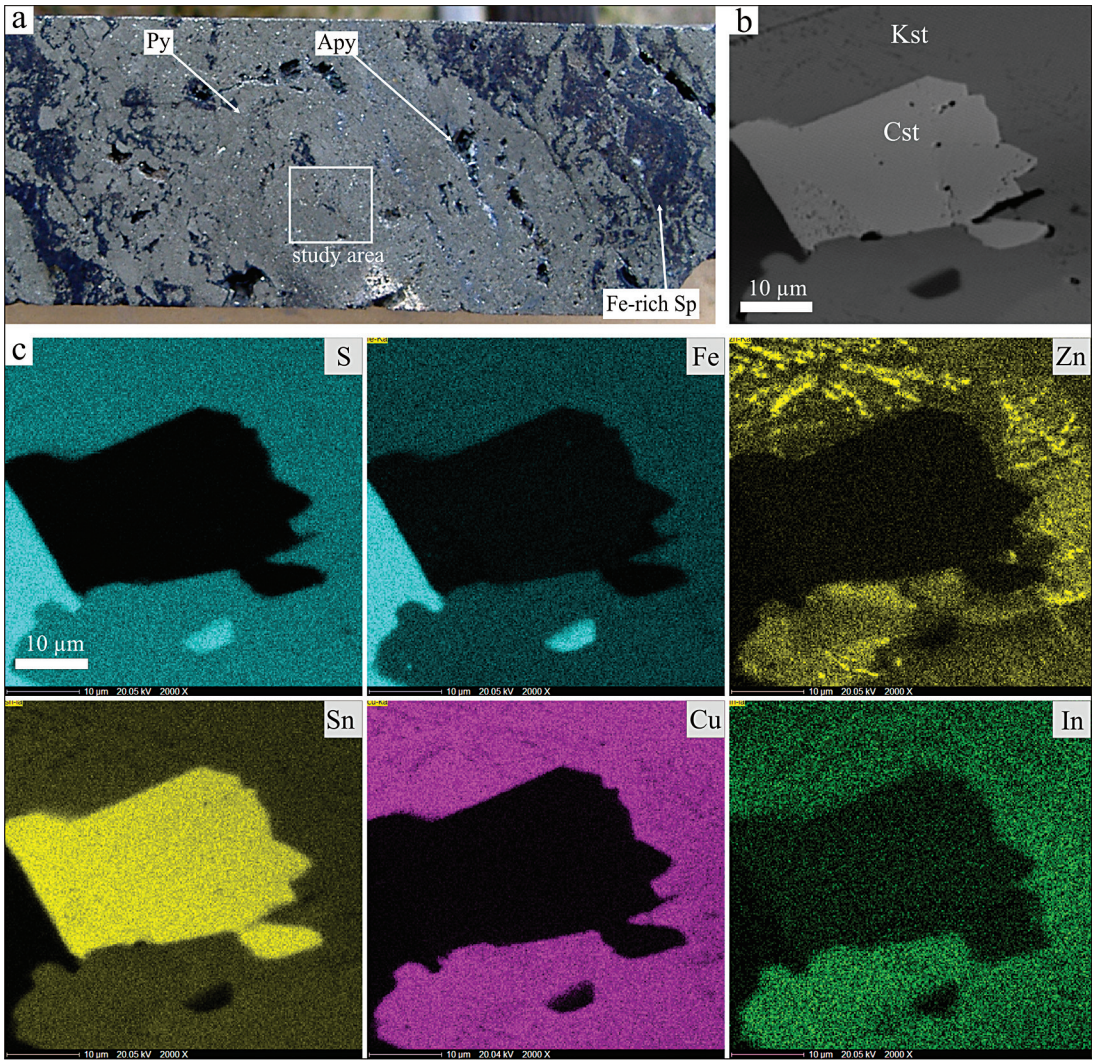

FIG. 8. (a) Representative sample of stage Ps_1 from the Ivonne vein (DDH–102; 53.3 meters below collar). Pyrite (Py) and arsenopyrite (Apy) cross-cut by Fe-rich sphalerite (Sp) and galena (Gn). Location of back-scattered image and quantitative electron-microprobe study is highlighted. (b) Back-scattered image of ferrokësterite (Fks) and cassiterite (Cst) crystals. (c) Element-distribution maps of (b) showing S, Fe, Zn, Sn, Cu and In.

chalcopyrite ($K\alpha$, LIF); Zn, sphalerite ($K\alpha$, LIF); As, GaAs ($K\beta$, TAP); Ag, Ag_2S ($K\alpha$, PET); Sn, cassiterite ($K\alpha$, PET); Sb, InSb ($K\alpha$, PET); Pb, galena ($M\alpha$, PET); Bi, BiSb ($L\alpha$, LIF); Mn, rhodonite ($K\alpha$, LIF); Ge, Ge metal ($K\alpha$, LIF); Cd, CdS ($K\alpha$, PET); In, InSb ($K\alpha$, PET); Ta, Ta metal ($K\alpha$, LIF); Ca, wollastonite ($K\alpha$, PET); W ($M\alpha$, TAP). Table 1 summarizes the results of the electron-microprobe analyses of the host minerals of indium from each stage, and Table 2 shows the indium content (wt.% In) of In-bearing minerals from each stage.

During the Ps_1 stage, the highest average content of In occurs in the ferrokësterite (0.51 wt.%, $n = 52$), followed by cassiterite and sphalerite (both with 0.22 wt.% on average, $n = 16$ and $n = 14$, respectively). Chalcopyrite does not concentrate significant amounts of In in this deposit. The variation of indium and other major and minor elements in ferrokësterite and cassiterite is shown as interelement plots in binary diagrams (Fig.

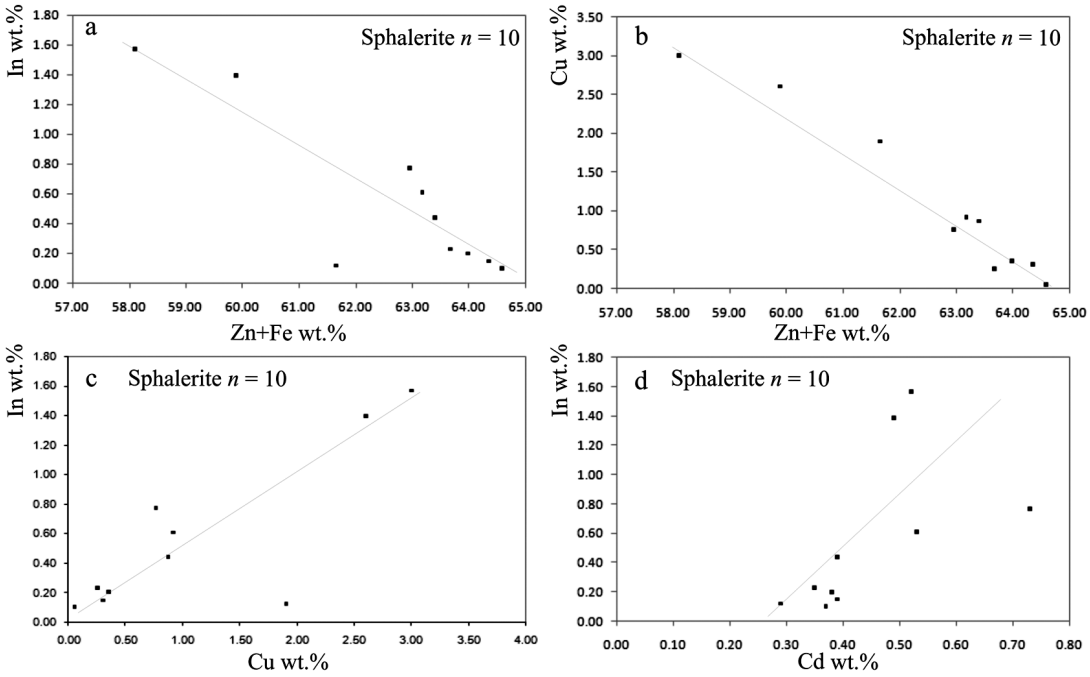

FIG. 9. Binary diagrams of Zn + Fe – In, Zn + Fe – Cu, Cd–In and Cu–In proportions in Fe-rich sphalerite; *n*: number of electron-microprobe measurements.

TABLE 1. COMPOSITION OF THE MAIN MINERALS FROM EACH STAGE OF MINERALIZATION

	Ps_1				Ps_2		Ps_3	
	Ccp	Cst	Fks	Sp	Sp	Fks	Sp	Gck
n	11	16	52	14	10	4	12	5
S wt.%	34.00		28.85	33.02	33.05	29.19	31.80	21.84
Mn	0.01	0.07	0.12	0.35	0.56	0.16	0.01	0.01
Fe	28.48	0.70	10.94	7.06	8.29	12.00	0.49	0.39
Zn	0.37		4.33	57.62	56.08	3.66	63.54	3.34
Ge	0.03		0.01	0.00				
Cd	0.02		0.09	0.43	0.50	0.05	0.52	71.98
In	0.06	0.22	0.51	0.22	0.47	0.09	0.06	3.07
Sn	0.71	78.06	26.22		0.52	26.88		
Cu	33.89		27.95		1.11	27.96		
Ag	0.06							
As	0.07							
Sb	0.04							
Pb	0.11							
Bi	0.23							
O		21.33						
Total	97.75	100.38	99.04	98.70	100.68	99.99	96.42	100.64

The data were acquired with an electron microprobe; *n*: number of electron-microprobe measurements. Three stages of mineralization were identified: polymetallic stage 1 (Ps_1), polymetallic stage 2 (Ps_2), and polymetallic stage 3 (Ps_3). Symbols used: Ccp: chalcopyrite, Cst: cassiterite, Fks: ferrokësterite, Sp: sphalerite, Gck: greenockite.

TABLE 2. INDIUM CONTENT OF HOST MINERALS FROM POLYMETALLIC STAGE 1 (Ps_1), POLYMETALLIC STAGE 2 (Ps_2), AND POLYMETALLIC STAGE 3 (Ps_3)

	Ps_1			Ps_2		Ps_3
	Cst	Fks	Sp	Sp	Fks	Gck
n	16	52	14	10	4	5
Average	0.22	0.51	0.22	0.47	0.09	3.07
Minimum	0.14	0.04	0.11	0.01	0.04	1.92
Maximum	0.36	3.02	0.55	2.56	0.16	3.63

Symbols used: Cst: cassiterite, Fks: ferrokësterite, Sp: sphalerite, Gck: greenockite. The indium contents are expressed in wt.% In. *n*: number of electron-microprobe measurements.

7). The indium concentration in ferrokësterite presents a negative correlation with tin (r = –0.78, n = 52; Fig. 7a) and copper contents (r = –0.71, n = 52; Fig. 7b), indicating structural substitution of Sn and Cu for In, whereas in cassiterite, the amount of indium is strongly correlated with iron (r = 0.85, n = 16; Fig. 7c) and correlated negatively with tin (r = –0.80, n = 16; Fig. 7d), reflecting substitution of Sn for In and Fe. In Figure 8, representative element-distribution maps of ferrokësterite and cassiterite (Fig. 8b) indicate the spatial

distribution of S, Fe, Zn, Sn, Cu, and In concentrations in the crystals. Clearly, the highest indium contents are heterogeneously distributed in the ferrokësterite (Figs. 4e, 8c), whereas in the cassiterite, the indium contents are lower but homogeneously distributed (Fig. 8c).

The indium concentration in Ps_2 (Tables 1, 2) is associated mainly with sphalerite (0.47 wt.%, $n = 10$) and, to a lesser extent, with ferrokësterite (0.09 wt.%, $n = 4$). The sphalerite shows an average Cu content of 1.11 wt.%, and significant Cd contents, 0.50 wt.%. This iron-rich sphalerite (8.29 wt.% Fe, $n = 10$) is characterized by In contents between 0.01 and 2.56 wt.%. A negative correlation exists between Zn + Fe and In ($r = –0.87$, $n = 10$; Fig. 9a), Zn + Fe with Cu ($r = –0.98$, $n = 10$; Fig. 9b) and Zn + Fe and Cd ($r = –0.27$, $n = 10$), whereas the In concentration correlates positively with Cu ($r = 0.82$, $n = 10$; Fig. 9c) and Cd ($r = 0.60$, $n = 10$; Fig. 9d). These correlations reflect a structural substitution of In, Cu and minor Cd in sphalerite, for example a coupled substitution of 2(Zn,Fe) for CuIn (Johan 1988, Ohta 1989, Sinclair *et al*. 2006). Element-distribution maps of a sphalerite crystal with an incipient zonation of light and dark alternating bands (Fig. 10b) shows high levels of In concentrated mainly in the light bands (Figs. 10b, c). The Zn and Fe contents are homogeneously distributed within the crystal, but with lower contents in the In-rich bands (Fig. 10c), whereas Sn in relatively high contents is related to the In-rich bands. The Cd distribution is not involved with the zonation bands and presents a homogeneous distribution (Fig. 10c).

Assemblage Ps_3 contains the highest In contents (Tables 1, 2), but in this case related with greenockite; values range between 1.92 and 3.63 wt.% (3.07 wt.% on average, $n = 5$). The sphalerite of this stage shows very low Fe values (0.49 wt.% on average, $n = 12$) and only traces of In (0.06 wt.% on average, $n = 12$) in comparison with the sphalerite of Ps_1 and Ps_2 assemblages (Table 1). A quantitative element-distribution image (Fig. 11) of botryoidal banded greenockite and Fe-poor sphalerite shows a concentration of In and Cd in the greenockite crystals and bands (Fig. 11c), and trace values of In in the Fe-poor sphalerite and pyrite. A negative correlation exists between In and Cd, reflecting a substitution relationship between them (Fig. 12).

Discussion

Indium-bearing polymetallic vein-type deposits are characterized worldwide by multistage infilling of veins and a characteristic zonation of minerals, resulting in mineralogically complex ores with intense telescoping. The mineralogy of indium is dominated by solid solutions with sphalerite, stannite, ferrokësterite, cassiterite, chalcopyrite, tetrahedrite, and minor roquesite, roquesite–sphalerite solid solution and sakuraiite (Schwarz-Schampera & Herzig 2002).

Ohta (1995) defined a common sequence of mineralization stages for the In–polymetallic deposits from Japan and Bolivia, with distinct geochemical signatures: an early Sn–W stage with cassiterite, minerals of the wolframite series, arsenopyrite and minor pyrrhotite, a Sn–In stage characterized by stannite, chalcopyrite and minor marcasite and sphalerite, and an Ag–Pb–Sn stage with Ag sulfosalts and minor Ag–Sn and Pb–Sn minerals. The most important minerals of indium are Fe-rich sphalerite and an unnamed Zn–In mineral that forms a continuous solid-solution with sphalerite and minor minerals of Sn (Ohta 1989). In fact, the mineral parageneses of the tin belt in Bolivia are similar to those found in Pingüino area. Keutsch & de Brodtkorb (2008) described the occurrence of ferrokësterite–kësterite as an important constituent of the San José mine in Oruro, Bolivia, but they did not provide data about the In content of this mineral.

In the Freiberg district, Germany, the polymetallic sulfide vein-type mineralization is characterized by As(–Au)–Zn–Cu(–In–Cd)–Sn–Pb–Ag–Bi–Sb in anomalous concentrations, with arsenopyrite, pyrite or marcasite (minor native Au), pyrrhotite, mostly Fe-rich sphalerite, stannite, chalcopyrite, cassiterite, tetrahedrite, bornite, and galena (Seifert & Sandmann 2006). Three mineral sequences were recognized: an early Fe–As sequence, a Zn–Sn–Cu sequence with a high concentration of In (the indium stage) and a late Pb–Ag sequence. Iron-rich sphalerite from the Zn–Sn–Cu stage is the most important indium-bearing mineral, characterized by In contents between 0.03 and 0.38 wt.%. However, some small grains of undetermined Zn–Cu–Sn–In–S minerals have contents of In between 1.3 to 2.9 wt.%.

Polymetallic mineralization in the Pingüino deposit presents similarities in the geochemical signature and mineralogy with these indium-bearing polymetallic veins from Japan, Bolivia and Germany. Moreover, the distribution of In among the minerals also is similar: In is concentrated in Sn minerals in the early stage (Ps_1) and in sphalerite in a later stage (Ps_2). The different mode of accommodation of In during the different stages may be related with changes in temperature.

During the first stage, In is homogeneously distributed in cassiterite but heterogeneously distributed in ferrokësterite. This fact suggests the existence of exsolution-induced domains at a submicroscopic scale. The extent of solid solution among ferrokësterite–kësterite and other stannite-group minerals has long been discussed (*i.e.,* Kissin 1989, Bonazzi *et al*. 2003). However, the role of In in these structures is not yet well understood, although high contents of this element seem to be a key in the stabilization of the structure of petrukite (Kissin & Owens 1989). Petrukite is chemically similar to ferrokësterite but is richer in indium and has a different structure. Hence, these exsolution-induced domains presumably are due to a miscibility gap between ferrokësterite and petrukite.

During the second stage, the zonal substitution of In + Cu in sphalerite can be attributed to changes in

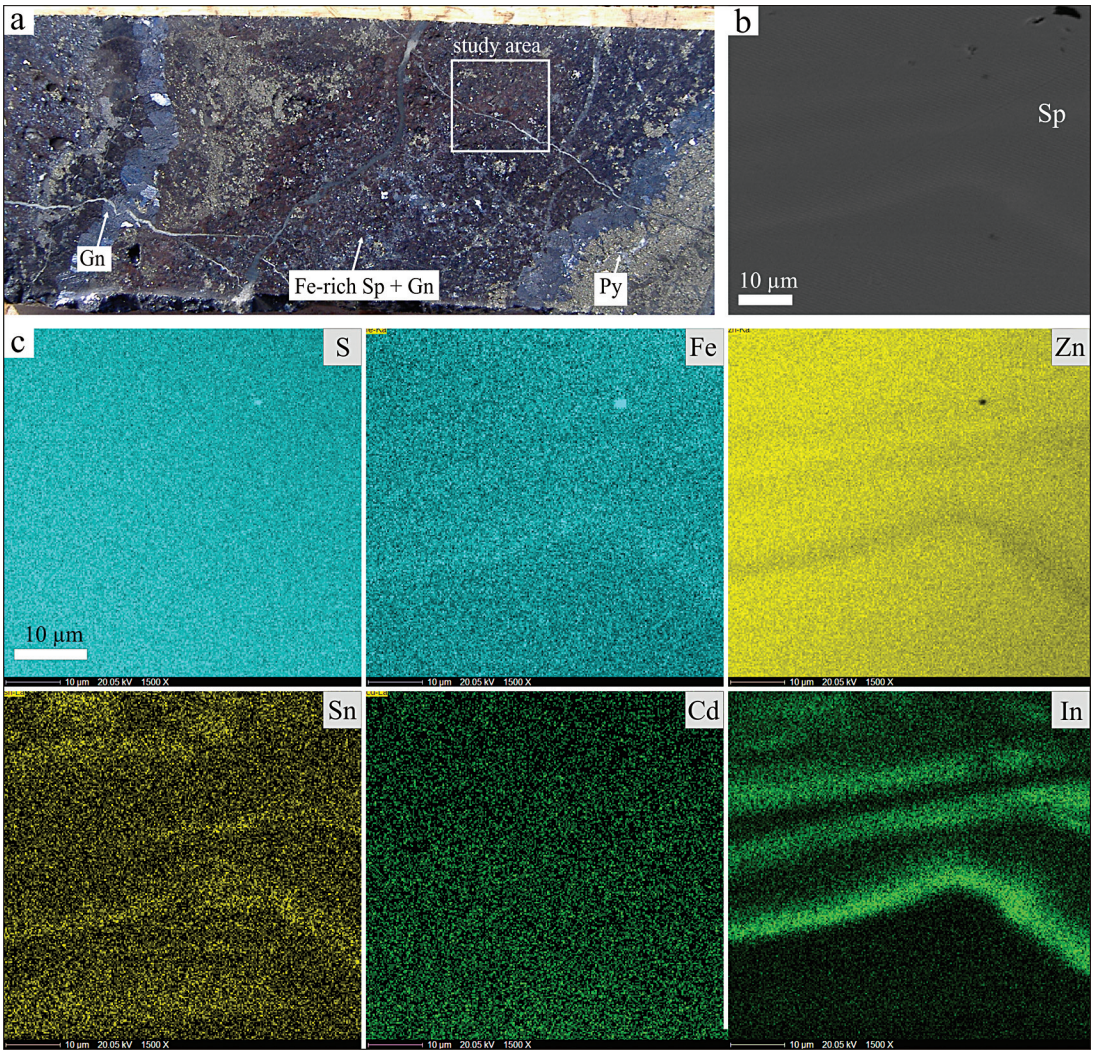

FIG. 10. (a) Representative sample of stage Ps_2 from the Marta Centro vein (DDH–53, 54.2 meters below collar). Banded Fe-rich sphalerite (Sp) and galena (Gn) breccia with pyrite (Py) clasts. Location of back-scattered image and quantitative electron-microprobe study is highlighted. (b) Back-scattered image of banded Fe-rich sphalerite (Sp) crystal. (c) Element-distribution maps of (b) showing S, Fe, Zn, Sn, Cu and In.

pH during crystallization (Pattrick *et al.* 1993), which are more likely than late diffusion of In + Cu (Oen *et al.* 1980, Doering *et al.* 1994). Furthermore, textures indicative of sphalerite replacement by Sn–In sulfosalts, such as those described in Redziny in Poland (Pieczka *et al.* 2009), are lacking in Pingüino. It is also important to note that the In content is very high in comparison with the average of most of worldwide deposits, but it is far from the highest contents of In ever found in a vein-type deposit, 6.7 wt.% (Cook *et al.* 2009).

On the other hand, although the third stage (Ps_3) is volumetrically not important, it is important to note that at least at low temperatures, In prefers the greenockite structure to sphalerite. Greenockite crystals are commonly found as a late mineral in the Sn-bearing polymetallic veins deposits of Bolivia (*i.e.*, Ahlfeld 1951). Hence, a detailed geochemical study of these late stages can provide new data about the distribution of In at low temperatures. Also, it should be noted that deposits of this type are related to felsic igneous rocks, either plutonic or volcanic. In the Pingüino case,

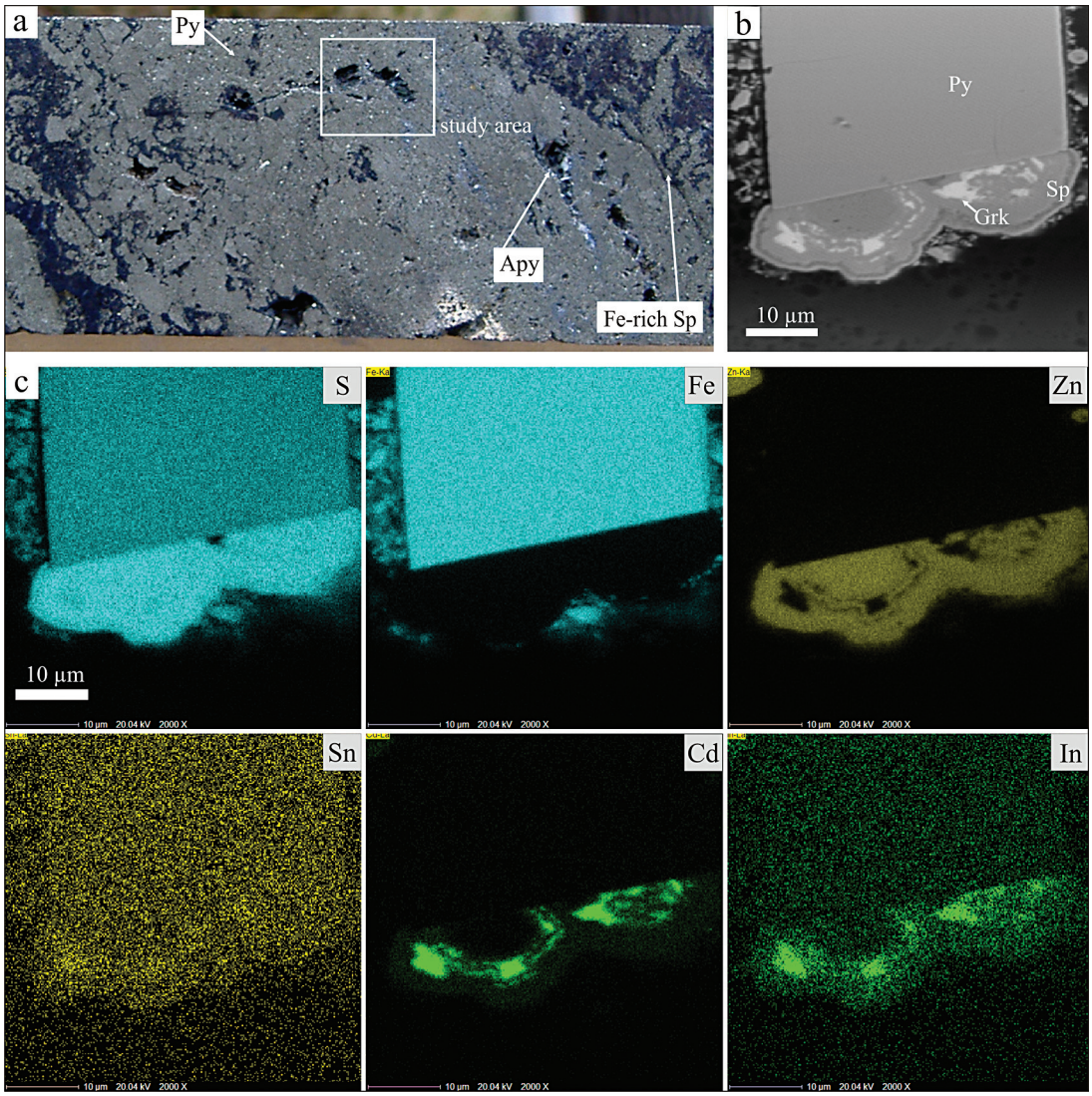

FIG. 11. (a) Representative sample of stage Ps_3 from the Ivonne vein (DDH–102; 53.3 meters below collar). Pyrite (Py) and arsenopyrite (Apy) cross-cut by Fe-rich sphalerite (Sp). Location of back-scattered image and quantitative electron-microprobe study is highlighted. (b) Back-scattered image of botryoidal banded of greenockite (Grk) and Fe-poor sphalerite (Sp) and pyrite (Py) crystal. (c) Element-distribution maps of (b) showing S, Fe, Zn, Sn, Cu and In.

although these rocks do not outcrop, the domal structure of the area and the fractures have been attributed to a shallow (1.5 km) intrusion. Hence, the Pingüino veins can represent the distal part of a peribatholithic hydrothermal system.

CONCLUSIONS

1) The polymetallic mineralization from Pingüino deposit results in high In values (up to 1184 ppm), representing an indium ore, and could be defined as an indium-bearing polymetallic vein deposit.

2) The mineral sequence in the veins indicates the existence of three main stages. At the first stage, rich in Sn and formed at higher temperature, the In is

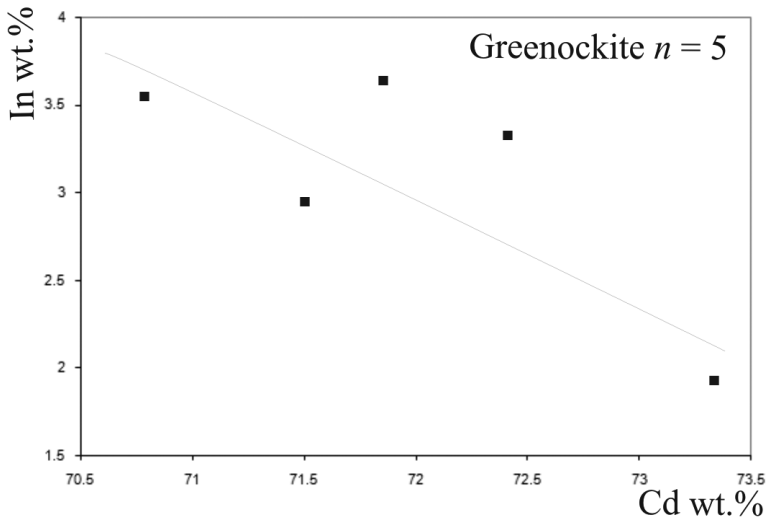

FIG. 12. Binary diagram of In–Cd proportions in greenockite; *n*: number of electron-microprobe measurements.

fractionated into Sn minerals (ferrokësterite and cassiterite). At the second stage, In is concentrated in Fe-rich sphalerite. During the third stage, formed at lower temperatures, greenockite crystals are the main carrier of indium. Hence, the distribution of In among the mineral species seems to be controlled by temperature.

3) The presence of high values of In mainly and also of Zn, Pb, Ag, Au, Cu, Sn, W and Bi in the polymetallic veins of the Pingüino vein system opens interesting possibilities for mineral exploration in the Deseado Massif.

ACKNOWLEDGEMENTS

We thank Ken Hicks and Argentex Mining Corporation for their constant support. We also appreciate the support, discussions and constructive suggestions given by Miguel Del Blanco, Anna Crespi and Joaquín Proenza. The microprobe analyses were obtained at the Serveis Científico-Tècnics de la Universitat de Barcelona (Xavier Llovet, analyst), as well as the SEM images. Some funds were provided by the project SGR589 and SGR444 of the Generalitat de Catalunya. María Florencia Marquéz-Zavalia and Robert F. Martin are thanked for very constructive reviews.

REFERENCES

AHLFELD, F. (1951): A new locality for greenockite crystals in Bolivia. *Am. Mineral.* **36**, 165-166.

ARGENTEX MINING CORPORATION (2009): National Instrument 43-101-compliant mineral resource estimate. http://www.argentexmining.com.

BARTON, P.B., JR. & BETHKE, P.M. (1987): Chalcopyrite disease in sphalerite: pathology and epidemiology. *Am. Mineral.* **72**, 451-467.

BENZAAZOUA, M., MARION, P., PINTO, A., MIGEON, H. & WAGNER, F.E. (2003): Tin and indium mineralogy within selected samples from the Neves Corvo ore deposit (Portugal): a multidisciplinary study. *Minerals Engineering* **16**(11, Suppl.), 1291-1302.

BINNS, R.A. & SCOTT, S.D. (1993): Actively forming polymetallic sulfide deposits associated with felsic volcanic rocks in the eastern Manus back-arc basin, Papua New Guinea. *Econ. Geol.* **88**, 2226-2236.

BONAZZI, P., BINDI, L., BERNARDINI, G.P. & MENCHETTI, S. (2003): A model for the mechanism of incorporation of Cu, Fe and Zn in the stannite–kësterite series, Cu_2FeSnS_4–Cu_2ZnSnS_4. *Can. Mineral.* **41**, 639-647.

BOORMAN, R.S. & ABBOTT, D. (1967): Indium in co-existing minerals from the Mount Pleasant tin deposit. *Can. Mineral.* **9**, 166-179.

BURKE, E.A.J. & KIEFT, C. (1980): Roquesite and copper–indium-bearing sphalerite from Långban, Bergslagen, Sweden. *Can. Mineral.* **18**, 361-363.

CARRILLO-ROSÚA, J., MORALES-RUANO, S. & FENOLL, P.H.-A. (2008): Textural and chemical features of sphalerite from

the Palai–Islica deposit (SE Spain): implications for ore genesis and color. *Neues Jahrb. Mineral., Abh.* **185**, 63-78.

COOK, N.J., CIOBANU, C.L., PRING, A., SKINNER, W., SHIMIZU, M., DANYUSHEVSKY, L., SAINI-EIDUKAT, B. & MELCHER, F. (2009): Trace and minor elements in sphalerite: a LA–ICPMS study. *Geochim. Cosmochim. Acta* **73**, 4761-4791.

CORTIÑAS, J., HOMOVC, J., LUCERO, M., GOBBO, E., LAFFITTE, G. & VIERA, A. (2005): Las cuencas de la región del Deseado, provincia de Santa Cruz. *In* Frontera Exploratoria de la Argentina (A.G. Chebli, J.S. Cortiñas, L.A. Spalletti, L. Legarreta & E.L. Vallejo, eds.). 1st ed. Instituto Argentino del Petróleo y del Gas, Buenos Aires, Argentina (289-305).

CRESPI, A. (2006): Estudi mineralògic dels dipòsits del massís de El Deseado (Argentina). Bachelor's thesis, Univ. de Barcelona, Barcelona, Spain.

CRESPI, A., JOVIC, S.M., GUIDO, D.M., PROENZA, J., MELGAREJO, J.C. & SCHALAMUK, I.B. (2006): El prospecto Cerro León, Macizo del Deseado, Patagonia, Argentina: un depósito de Ag–Sn. *Macla* **6**, 143-145.

DOERING, T., KAEMPF, H. & BENTE, K. (1994): Disease phenomena in In-bearing sphalerite from Oelsnitz/Vogtland (Germany): a comparison of natural and experimental textures and their application to ore mineral genesis. *In* Metallogeny of Collisional Orogens Focussed on the Erzgebirge and Comparable Metallogenic Settings (R. Seltmann, H. Kämpf & P. Möller, eds.). Czech Geol. Surv., Prague, Czech Republic (103-109).

FOUQUET, Y., VON STACKELBERG, U., CHARLOU, J.L., ERZINGER, J., HERZIG, P.M., MUEHE, R. & WIEDICKE, M. (1993a): Metallogenesis in back-arc environments: the Lau basin example. *Econ. Geol.* **88**, 2154-2181.

FOUQUET, Y., WAFIK, A., CAMBON, P., MÉVEL, C., MEYER, G. & GENTE, P. (1993b): Tectonic setting and mineralogical and geochemical zonation in the Snake Pit sulfide deposit (Mid-Atlantic Ridge at 23°N). *Econ. Geol.* **88**, 2018-2036.

GORELIKOVA, N., TOLOSANA-DELGADO, R., PAWLOWSKY-GLAHN, V., KHANCHUK, A. & GONEVCHUK, V. (2006): Discriminating geodynamical regimes of tin ore formation using trace element composition of cassiterite: the Sikhote' Alin case (Far Eastern Russia). *In* Compositional Data Analysis in the Geosciences: from Theory to Practice (A. Buccianti, G. Mateu-Figueras & V. Pawlowsky-Glahn, eds.). *Geol. Soc., Spec. Publ.* **264**, 43-57.

GUIDO, D.M., JOVIC, S.M. & SCHALAMUK, I.B. (2005): A new metallogenic association (Sn–Cd–In–Zn–Ag–Au) in the Deseado auroargentiferous province, Deseado Massif, Patagonia, Argentina. *In* Mineral Deposit Research: Meeting the Global Challenge **2** (J. Mao & F.P. Bierlein, eds.). *Proc. Eighth Biennial SGA Meeting* (*Beijing*) (965-968).

GUIDO, D.M. & SCHALAMUK, I.B. (2003): Genesis and exploration potential of epithermal deposits from the Deseado Massif, Argentinean Patagonia. *In* Mineral Exploration and Sustainable Development **I** (D. Eliopoulos, ed.). Balkema, Rotterdam, The Netherlands (493-496).

HERBST, R. (1965): La flora fósil de la Formación Roca Blanca, provincia de Santa Cruz, Patagonia, con consideraciones geológicas y estratigráficas. *Opera Lilloana* **12**, 1-102.

HUSTON, D.L., SIE, SOEY H., SUTER, G.F., COOKE, D.R. & BOTH, R.A. (1995): Trace elements in sulfide minerals from eastern Australian volcanic-hosted massive sulfide deposits. I. Proton microprobe analyses of pyrite, chalcopyrite and sphalerite. II. Selenium levels in pyrite: comparison with $\delta^{34}S$ values and implications for the source of sulfur in volcanogenic hydrothermal systems. *Econ. Geol.* **90**, 1167-1196.

ISHIHARA, S., HOSHINO, K., MURAKAMI, H. & ENDO, Y. (2006): Resource evaluation and some genetic aspects of indium in the Japanese ore deposits. *Resource Geol.* **56**, 347-364.

JALFIN, G. & HERBST, R. (1995): La flora triásica del Grupo El Tranquilo, provincia de Santa Cruz (Patagonia). Estratigrafía. *Ameghiniana* **32**, 211-229.

JOHAN, Z. (1988): Indium and germanium in the structure of sphalerite: an example of coupled substitution with copper. *Mineral. Petrol.* **39**, 211-229.

JOVIC, S.M. (2010): Geología y metalogénesis de las mineralizaciones polimetálicas del área El Tranquilo (Cerro León), sector central del Macizo del Deseado, Provincia de Santa Cruz. (1ra ed.) *Editorial de la Universidad de La Plata (EDULP)*, La Plata, Argentina.

JOVIC, S.M., GUIDO, D.M., PÁEZ, G.N., LÓPEZ, R.G. & SCHALAMUK, I.B. (2006): Marco estructural de las mineralizaciones polimetálicas del área del anticlinal El Tranquilo, Macizo del Deseado, Santa Cruz. *13° Reunión de Tectónica*, Actas en CD.

JOVIC, S.M., GUIDO, D.M., RUIZ, R., PÁEZ, G.N. & SCHALAMUK, I.B. (2011b): Indium distribution and correlations in polymetallic veins from Pingüino deposit, Deseado Massif, Patagonia, Argentina. *Geochemistry: Exploration, Environment, Analysis* **11**, 107-115.

JOVIC, S.M., GUIDO, D.M., SCHALAMUK, I.B., MELGAREJO, J.C. & PROENZA, J. (2005): Mineralogía de veta Ivonne, deposito Cerro León: ¿Paragénesis de alta temperatura en la Provincia Auroargentifera del Deseado? *XVI Congreso Geológico Argentino. Actas* **2**, 257-262.

JOVIC, S.M., GUIDO, D.M., SCHALAMUK, I.B., RÍOS, F.J., TASSINARI, C.C.G. & RECIO, C. (2011a): Pingüino In-bearing polymetallic vein deposit, Deseado Massif, Patagonia, Argentina: characteristics of mineralization and ore-forming fluids. *Miner. Deposita* **46**, 257-271.

KEUTSCH, F. & DE BRODTKORB, M.K. (2008): Metalliferous paragenesis of the San José mine, Oruro, Bolivia. *J. S. Am. Earth Sci.* **25**, 485-491.

KIEFT, K. & DAMMAN, A.H. (1990): Indium-bearing chalcopyrite and sphalerite from the Gåsborn area, West Bergslagen, central Sweden. *Mineral. Mag.* **54**, 109-112.

KISSIN, S.A. (1989): A reinvestigation of the stannite (Cu_2FeSnS_4) – këwhile (Cu_2ZnSnS_4) pseudobinary system. *Can. Mineral.* **27**, 689-697.

KISSIN, S.A. & OWENS, D.R. (1989): The relatives of stannite in the light of new data. *Can. Mineral.* **27**, 673-688.

LENHARO, S.L.R., MOURA, M.A. & BOTELHO, N.F. (2002): Petrogenetic and mineralization processes in Paleo- to Mesoproterozoic rapakivi granites: examples from Pitinga and Goias, Brazil. *Precamb. Res.* **119**, 277-299.

LEROUGE, C., DESCHAMPS, Y., PIANTONE, P., GILLES, C. & BRETON, J. (2007): Metal-carrier accessory minerals associated with W±Sn mineralization, La Châtaigneraie tungsten ore district, Massif Central, France. *Can. Mineral.* **45**, 875-889.

MOURA, M.A., BOTELHO, N.F. & CARVALHO DE MENDONÇA, F. (2007): The indium-rich sulfides and rare arsenates of the Sn–In ore-mineralized Mangabeira A-type granite, central Brazil. *Can. Mineral.* **45**, 485-496.

OEN, I.S., KAGER, P. & KIEFT, C. (1980): Oscillatory zoning of a discontinuous solid-solution series: sphalerite–stannite. *Am. Mineral.* **65**, 1220-1232.

OHTA, E. (1989): Occurrence and chemistry of indium-containing minerals from the Toyoha mine, Hokkaido, Japan. *Mining Geol.* **39**, 355-372.

OHTA, E. (1995): Common features and genesis of tin–polymetallic veins. *Resource Geol., Spec. Issue* **18**, 187-195.

PALERO-FERNÁNDEZ, F.J. & MARTÍN-IZARD, A. (2005): Trace element contents in galena and sphalerite from ore deposits of the Alcudia Valley mineral field (eastern Sierra Morena, Spain). *J. Geochem. Explor.* **86**, 1-25.

PANZA, J. (1995): Hoja geológica 4969 – II Tres Cerros escala 1: 250.000, provincia de Santa Cruz. *Dirección Nacional del Servicio Geológico*, *Boletín* **213**, 1-103.

PATTRICK, R.A.D., DORLING, M. & POLYA, D.A. (1993): TEM study of indium- and copper-bearing growth-banded sphalerite. *Can. Mineral.* **31**, 105-117.

PEÑALVA, G.A., JOVIC, S.M., CHERNICOFF, C.J., GUIDO, D.M. & SCHALAMUK, I.B. (2008): Cuerpos intrusivos asociados a las mineralizaciones polimetálicas del depósito Cerro León, área del anticlinal El Tranquilo, Santa Cruz: evidencias geofísicas. *Rev. Asoc. Geol. Argentina* **63**, 14-23.

PIECZKA, A., GOLEBIOWSKA, B. & PARAFINIUK, J. (2009): Conditions of formation of polymetallic mineralization in the eastern envelope of the Karkonosze granite: the case of Redziny, southwestern Poland. *Can. Mineral.* **47**, 765-786.

PLIMER, I.R., LU, J. & KLEEMAN, J.D. (1991): Trace and rare earth elements in cassiterite. Sources of components for the tin deposits of the Mole Granite, Australia. *Mineral. Deposita* **26**, 267-274.

QIAN, Z., ZHAN, X., PAN, J. & SHAO, S. (1998): Geochemical enrichment and mineralization of indium. *Chin. J. Geochem.* **17**, 221-225.

SCHWARZ-SCHAMPERA, U. & HERZIG, P.M. (1997): Geochemistry of indium in VMS deposits. Implications from active hydrothermal vents in the southern Lau Basin (SW-Pacific). *In* Mineral Deposits: Research and Exploration, Where Do They Meet? (H. Papunen, ed.). A.A. Balkema, Rotterdam, the Netherlands (379-382).

SCHWARZ-SCHAMPERA, U. & HERZIG, P. (2002): *Indium. Geology, Mineralogy, and Economics*. Springer-Verlag, Berlin, Germany.

SEIFERT, T. (1999): Relationship between the Late Variscan lamprophyres and hydrothermal vein mineralization in the Erzgebirge. *In* Mineral Deposits: Processes to Processing **1** (C.J. Stanley, ed.). A.A. Balkema, Rotterdam, the Netherlands (429-432).

SEIFERT, T. & SANDMANN, D. (2006): Mineralogy and geochemistry of indium-bearing polymetallic vein-type deposits: implications for host minerals from the Freiberg district, eastern Erzgebirge, Germany. *Ore Geol. Rev.* **28**, 1-31.

SERRANTI, S., FERRINI, V., MASI, U. & CABRI, L.J. (2002): Trace-element distribution in cassiterite and sulfides from rubané and massive ores of the Corvo deposit, Portugal. *Can. Mineral.* **40**, 815-835.

SHIMIZU, M. & KATO, A. (1991): Roquesite-bearing tin ores from the Omodani, Akenobe, Fukoku, and Ikuno polymetallic vein-type deposits in the Inner Zone of southwestern Japan. *Can. Mineral.* **29**, 207-215.

SINCLAIR, W.D., KOOIMAN, G.J.A., MARTIN, D.A. & KJARSGAARD, I.M. (2006): Geology, geochemistry and mineralogy of indium resources at Mount Pleasant, New Brunswick, Canada. *Ore Geol. Rev.* **28**, 123-145.

TSUSHIMA, N., MATSUEDA, H. & ISHIHARA, S. (1999): Polymetallic mineralization at the Nakakoshi copper deposits, central Hokkaido, Japan. *Resource Geol.* **49**, 89-97.

ZHANG, QIAN, ZHU, XIAOQING, HE, YULIANG, JIANG, JUNJIE & WANG, DAPENG (2006): Indium enrichment in the Meng'entaolegai Ag–Pb–Zn deposit, Inner Mongolia, China. *Resource Geol.* **56**, 337-346.

ZHANG, QIAN, ZHU, XIAOQING, HE, YULIANG & ZHU, Z. (2007): In, Sn, Pb and Zn contents and their relationships in ore-forming fluids from some In-rich and In-poor deposits in China. *Acta Geol. Sinica* **81**, 450-462.

Received July 8, 2010, revised manuscript accepted July 9, 2011.